

Polar phonons and spin-phonon coupling in HgCr_2S_4 and CdCr_2S_4 studied with far-infrared spectroscopy

T. Rudolf,¹ Ch. Kant,¹ F. Mayr,¹ J. Hemberger,¹ V. Tsurkan,^{1,2} and A. Loidl¹

¹*Experimental Physics V, Center for Electronic Correlations and Magnetism, University of Augsburg, D-86135 Augsburg, Germany*

²*Institute of Applied Physics, Academy of Sciences of Moldova, MD-2028 Chişinău, Republic of Moldova*

(Received 25 July 2007; published 30 November 2007)

Polar phonons of HgCr_2S_4 and CdCr_2S_4 are studied by far-infrared spectroscopy as a function of temperature and external magnetic field. Eigenfrequencies, damping constants, effective plasma frequencies, Lyddane-Sachs-Teller relations, and effective charges are determined. Ferromagnetic CdCr_2S_4 and antiferromagnetic HgCr_2S_4 behave rather similar. Both compounds are dominated by ferromagnetic exchange, and although HgCr_2S_4 is an antiferromagnet, no phonon splitting can be observed at the magnetic phase transition. Temperature and magnetic-field dependencies of the eigenfrequencies show no anomalies, indicating dispersive polar soft-mode behavior. However, significant effects are detected in the temperature dependence of the plasma frequencies, indicating changes in the nature of the bonds and significant charge transfer. In HgCr_2S_4 , we provide experimental evidence that the magnetic-field dependence of specific polar modes reveals shifts exactly correlated with the magnetization, showing significant magnetodielectric effects even at infrared frequencies.

DOI: [10.1103/PhysRevB.76.174307](https://doi.org/10.1103/PhysRevB.76.174307)

PACS number(s): 63.20.-e, 75.50.Ee, 78.30.-j

I. INTRODUCTION

In the chromium spinels $A\text{Cr}_2X_4$ ($A=\text{Zn}, \text{Cd}, \text{Hg}; X=\text{O}, \text{S}, \text{Se}$), competing antiferromagnetic (AFM) and ferromagnetic (FM) interactions¹ establish a fascinating phase diagram with complex ground states.² In these compounds, the Cr^{3+} ions exhibit a half-filled t_{2g} shell constituting a spin-only state with $S=3/2$ and vanishing spin-orbit coupling.

The oxides, with small lattice constants, are dominated by direct AFM Cr-Cr exchange. As the chromium ions form a corner-sharing tetrahedral network, which is a prototypical example of a pyrochlore lattice, these compounds are geometrically frustrated³ and undergo antiferromagnetic spin order at temperatures $T \ll \Theta_{CW}$, where Θ_{CW} is the Curie-Weiss temperature. The magnetic transitions are accompanied by structural distortions which have been explained in terms of a spin-driven Jahn-Teller (JT) effect.^{4,5} In most of these AFM spinels, the phonon eigenmodes reveal significant splittings below the AFM ordering temperature.^{2,6-8} The phonon splittings are driven by magnetic exchange interactions via strong spin-phonon coupling, despite the fact that Cr^{3+} in an octahedral crystalline electric field reveals a spherical charge distribution with a g value close to $g=2$, synonymous with the absence of conventional spin-orbit coupling.

At large lattice constants, in some of the sulfides and selenides,^{1,2} 90° Cr-X-Cr exchange becomes dominant, leading to FM semiconductors with relatively high magnetic transition temperatures. Recently, relaxor ferroelectricity has been reported for CdCr_2S_4 (Ref. 9) and HgCr_2S_4 .¹⁰ This seems to be a further experimental evidence concerning the long-standing question of local polar distortions in spinel compounds.¹¹ However, the origin of these polar distortions is unclear,¹² and in *ab initio* phonon calculations,¹³ no indications for a structural instability due to soft phonon modes have been detected. Recently, evidence accumulates that the large magnetocapacitive (MC) effects in the chromium spinels strongly depend on thermal treatment and/or doping.

In pure ceramics, for example, MC effects are absent or strongly reduced, but they are recovered in indium doped samples. On the contrary, annealing in vacuum eliminates MC effects in Cl-doped single crystals but enables them in Cl-free single crystals.^{14,15} The observation that marginal doping with charge carriers induces dipolar relaxation phenomena reminds of similar effects in transition-metal monoxides doped on a subpercent level with Li (Ref. 16) or on metal deficient semiconducting NiO.¹⁷ Specifically, for MnO, it has been suggested that Li doping leads to Mn^{4+} ions with a strongly Jahn-Teller active d^4 electron configuration, inducing polaronlike bound charge carriers. In a similar way, CdCr_2S_4 with sulfur deficiency or doped with Cl^- will exhibit Cr^{2+} with a JT active d^4 configuration and possible dipolar relaxation of bound polarons. Additional experiments will be necessary to unravel if the observed relaxor phenomena can be explained by doping only or by intrinsic lattice instabilities driven by off centering of the Cr ions as has been proposed by recent Raman scattering experiments.¹⁸

It is known for a long time that in CdCr_2S_4 , strong spin-phonon coupling is active,¹⁹ leading to an unusual temperature dependence of eigenfrequencies and dampings of the infrared (IR) active phonon modes. In addition, recent Raman scattering experiments provide experimental evidence for polar distortions well above the magnetic ordering temperature.¹⁸ In this work, we communicate the results of a detailed IR study. We report on the temperature dependence of eigenfrequencies, dampings, and effective plasma frequencies of all IR active phonons in HgCd_2S_4 and CdCr_2S_4 . Our results show that while there are indeed no indications of strong phonon softening, we observe strong effects in the temperature dependence of the plasma frequencies of specific modes, indicative for significant changes of the character of bonds and that the effective charges undergo large variations as a function of temperature. In addition, it seems worthwhile to search for phonon splitting in AFM HgCr_2S_4 , as has been observed in the related Cr spinels ZnCr_2S_4 (Ref.

7) and ZnCr_2Se_4 (Ref. 8) below the antiferromagnetic phase-transition temperature. HgCr_2S_4 is close to FM order, and moderate magnetic fields well below 1 T induce a polarized ferromagnetic state which is shifted by almost 60 K in external fields of 5 T.²⁰ It thus seems particularly important to study the spin-phonon coupling also as function of an external magnetic field.

II. EXPERIMENTAL DETAILS

CdCr_2S_4 and HgCr_2S_4 crystallize in the normal cubic spinel structure ($Fd\bar{3}m$) with lattice constants $a=1.0247$ nm and $a=1.0256$ nm and sulfur fractional coordinates $x=0.263$ and $x=0.267$ for the cadmium and mercury compounds, respectively.² Both compounds are dominated by strong FM exchange with Curie-Weiss temperatures of the order of 150 K. However, while CdCr_2S_4 reveals FM order at $T_C=84.5$ K,^{2,9} HgCr_2S_4 exhibits spiral-like AFM spin order below 22 K.^{2,20,21}

The IR experiments on CdCr_2S_4 were performed on as-grown single crystals obtained by chemical transport reaction method using Cl as a transport agent. The measurements were repeated on high-purity ceramic samples to check for possible effects on the phonon properties by doping with chlorine. In the single crystals, a Cl concentration <0.25 mol % and a concomitant charge carrier density may be present, but from x-ray studies with synchrotron radiation, we can certainly exclude any clustering of Cl ions. From detailed wave length sensitive microprobe analysis, we are sure that single crystals and ceramics investigated in these studies are very close to ideal stoichiometry. Our IR results in CdCr_2S_4 are in good agreement with those reported by Wakamura and Arai¹⁹ on ceramic samples. CdCr_2S_4 reveals relaxor-type ferroelectric behavior below approximately 130 K. This glasslike transition is dynamic and strongly depends on the measuring frequency.⁹ Soft ferromagnetism with a fully developed magnetic moment of the chromium spins appears below 84.5 K. The measurements on HgCr_2S_4 , documented in this work, were made on ceramic pellets with polished surfaces. HgCr_2S_4 is dominated by strong ferromagnetic fluctuations²⁰ but undergoes AFM spin order below 22 K.^{10,20,21} Ferroelectric hysteresis loops have been reported close to 70 K, well above the AFM phase transition.¹⁰

The reflectivity measurements were carried out in the far-infrared range using the Bruker Fourier-transform spectrometer IFS 113v equipped with a He-bath cryostat and with a split-coil magnet for measurements in external magnetic fields up to 7 T. With this setup, we were able to measure the frequency range from 50 to 700 cm^{-1} with high precision. The reflectivity measurements were performed on polished surfaces of the samples. To get an independent estimate of the background dielectric constant, the static dielectric constant ϵ_0 has been measured for both compounds between 150 and 500 GHz using millimeter spectroscopy.²² In these measurements, the real and imaginary parts of the dielectric constant can be measured directly via transmission and phase shift, without relying on any Kramers-Kronig-type analysis for the calculation of the complex permittivity.

Room-temperature far-infrared spectra of HgCr_2S_4 and CdCr_2S_4 were published by Lutz *et al.*²³ and by Wakamura *et al.*^{19,24} Incomplete spectra of CdCr_2S_4 have also been published by Lee.²⁵ Some preliminary far-infrared results on HgCr_2S_4 have been published in Ref. 2. The temperature dependence of the phonon eigenfrequencies and dampings in CdCr_2S_4 has been reported by Wakamura and Arai.¹⁹ The present experiments were undertaken with special attention to search for fingerprints in the phonon spectra for a possible onset of ferroelectricity in both compounds and to search for phonon splittings in AFM HgCr_2S_4 , which could be expected on symmetry arguments alone. In addition, we also performed far-infrared measurements as function of external magnetic fields to search for magnetodielectric effects at far-infrared frequencies.

III. ANALYSIS OF THE RESULTS

A. Modeling of the far-infrared spectra

The phonon contribution of the complex dielectric function $\epsilon(\omega)=\epsilon_1(\omega)+i\epsilon_2(\omega)$ of an insulating crystal is obtained by calculating the factorized function

$$\epsilon(\omega) = \epsilon_\infty \prod_j \frac{\omega_{Lj}^2 - \omega^2 - i\gamma_{Lj}\omega}{\omega_{Tj}^2 - \omega^2 - i\gamma_{Tj}\omega}. \quad (1)$$

Here, ω_{Lj} , ω_{Tj} , γ_{Lj} , and γ_{Tj} correspond to longitudinal (L) and transversal (T) eigenfrequencies (ω_j) and dampings (γ_j) of mode j , respectively. ϵ_∞ results from high-frequency electronic absorption processes and can be experimentally determined from the reflectivity or the index of refraction at frequencies larger than the phonon eigenfrequencies. At normal incidence, $\epsilon(\omega)$ is related to the reflectivity $R(\omega)$ via

$$R(\omega) = \left| \frac{\sqrt{\epsilon(\omega)} - 1}{\sqrt{\epsilon(\omega)} + 1} \right|^2. \quad (2)$$

Using Eqs. (1) and (2), the reflectivity spectra can be unambiguously described using a four-parameter fit routine, which has been recently developed by Kuzmenko.²⁶ In most cases, when the modes are well separated, this fit allows a precise determination of ϵ_∞ , longitudinal and transversal eigenfrequencies (ω_{Lj} , ω_{Tj}), and dampings (γ_{Lj} , γ_{Tj}). Using this formalism, the dielectric strength $\Delta\epsilon$ can then be calculated via

$$\Delta\epsilon = \epsilon_0 - \epsilon_\infty = \sum_j \Delta\epsilon_j = \epsilon_\infty \left(\prod_j \frac{\omega_{Lj}^2}{\omega_{Tj}^2} - 1 \right), \quad (3)$$

where ϵ_0 corresponds to the static $\epsilon(\omega \rightarrow 0)$ dielectric constant and $\Delta\epsilon_j$ to the strength of mode j , which, in the case of nonoverlapping modes, can be explicitly derived:

$$\Delta\epsilon_j = \epsilon_\infty \frac{\omega_{Lj}^2 - \omega_{Tj}^2}{\omega_{Tj}^2} \prod_{i=j+1} \frac{\omega_{Li}^2}{\omega_{Ti}^2}. \quad (4)$$

Assuming that the damping of transversal and longitudinal optical phonons is identical, Eq. (1) reduces to

$$\epsilon(\omega) = \epsilon_\infty + \sum_j \frac{\omega_j^2 \cdot \Delta\epsilon}{\omega_j^2 - \omega^2 - i\gamma_j\omega}. \quad (5)$$

This is the well known Lorentzian line shape with three independent parameters. ω_j equals ω_{Tj} of the four-parameter model, and ϵ_∞ is an additional variable, which, of course, has to be considered in both models. The mode strength $\Delta\epsilon$ can be related to an effective “ionic” plasma frequency Ω with

$$\Delta\epsilon_j\omega_{Tj}^2 = \Omega_j^2. \quad (6)$$

The effective plasma frequency of an IR active mode j , Ω_j , can then be related to the eigenfrequencies via

$$\Omega_j^2 = (\omega_{Lj}^2 - \omega_{Tj}^2) \cdot \tilde{\epsilon}_\infty(j), \quad (7)$$

where $\tilde{\epsilon}_\infty$ is the appropriate high-frequency dielectric constant for mode j , including all ionic contributions of modes i with $i > j$ [see Eq. (4)]:

$$\tilde{\epsilon}_\infty(j) = \epsilon_\infty \prod_{i=j+1} \frac{\omega_{Li}^2}{\omega_{Ti}^2}. \quad (8)$$

Finally, the dielectric strength of all polar modes can be related to a sum over all effective plasma frequencies Ω_j with

$$\Omega^2 = \sum_j \Omega_j^2 = \sum_j \Delta\epsilon_j\omega_{Tj}^2. \quad (9)$$

In favorable cases, using Eqs. (5)–(7), the ionicity or covalency of bonds involved in polar modes can be calculated. This is possible on the basis of Eq. (6) if the pattern of displacements of a specific phonon mode is known from an eigenvector analysis. However, even if this is not the case, one can arrive at definite conclusions about the effective charge of an ion. It has been pointed out by Scott²⁷ and has later been applied by Wakamura *et al.*^{19,24,28} to spinel compounds that, for a multimode system, one can assume

$$\Omega^2 = \sum_j (\omega_{Lj}^2 - \omega_{Tj}^2) \tilde{\epsilon}_\infty(j) = \frac{\epsilon_\infty}{V\epsilon_{vac}} \sum_k \frac{(Z_k^*e)^2}{m_k}. \quad (10)$$

Here, V is the unit-cell volume, ϵ_{vac} the dielectric permittivity of free space, and Z_k^*e the effective charge of the k th ion contributing to a specific polar mode with mass m_k . The k sum is over all atoms in the unit cell. This equation has to be combined with the expression for lattice charge neutrality,

$$\sum_k Z_k^* = 0. \quad (11)$$

In ternary compounds, Eqs. (10) and (11) do not allow us to determine all charges of the ions unambiguously. In these cases, specific assumptions concerning the effective charges of at least one ion have to be made.^{19,24,28}

In the present investigation, we are also interested in possible soft-mode phenomena accompanying ferroelectric phase transitions. Hence, we will focus on the generalized Lyddane-Sachs-Teller (LST) relation, which can be written as

$$\epsilon_0 = \epsilon_\infty \prod_j \frac{\omega_{Lj}^2}{\omega_{Tj}^2}. \quad (12)$$

In the case of a soft transverse optic mode, the LST relation gives a diverging static dielectric constant, which is indeed observed in many proper ferroelectrics.

B. Temperature dependence of eigenfrequencies and dampings

1. Anharmonic effects

To get an estimate of the influence of the magnetic exchange interactions on the phonon properties, we tried to describe the purely anharmonic temperature dependence of eigenfrequencies and dampings by a simple model, assuming

$$\omega_{Tj} = \omega_{T0j} \left(1 - \frac{c_j}{\exp(\Theta/T) - 1} \right) \quad (13)$$

for the temperature dependence of the transverse eigenfrequencies and

$$\gamma_{Tj} = \gamma_{T0j} \left(1 + \frac{d_j}{\exp(\Theta/T) - 1} \right) \quad (14)$$

for the temperature dependence of damping due to canonical anharmonic effects.

ω_{Tj} and γ_{Tj} are eigenfrequency and damping of the transversal optical mode j , and Θ is the Debye temperature, which has been determined from an average of the four IR active phonon frequencies. For the analysis of the anharmonic contributions, Debye temperatures of 361 K (HgCr₂S₄) and 372 K (CdCr₂S₄) have been determined. ω_{T0j} and γ_{T0j} are the values of phonon frequency and damping of the transverse mode j at 0 K. c_j and d_j are mere fitting parameters determining the strength of the anharmonic contributions. Detailed calculations of temperature and frequency dependent anharmonic contributions to eigenfrequencies and dampings can be found in Ref. 29.

2. Spin-phonon coupling

The spin-phonon coupling in magnetic semiconductors has been described by Baltensperger and Helman,³⁰ Baltensperger,³¹ Brüesch and D’Ambrogio,³² Lockwood and Cottam,³³ and Wesselinowa and Apostolov.³⁴ These authors have shown that the frequency shift of a given phonon mode as function of temperature is determined by a spin-correlation function

$$\omega = \omega_0 + \lambda \langle S_i \cdot S_j \rangle. \quad (15)$$

Here, ω is the renormalized phonon frequency, ω_0 denotes the eigenfrequency in the absence of spin-phonon coupling, and λ is the spin-phonon coupling constant. On the basis of these theories, Wakamura and Arai¹⁹ attempted to describe the experimentally observed frequency shifts $\Delta\omega$ in CdCr₂S₄ by taking into account a sum of two terms, namely, due to FM and AFM exchanges, respectively,

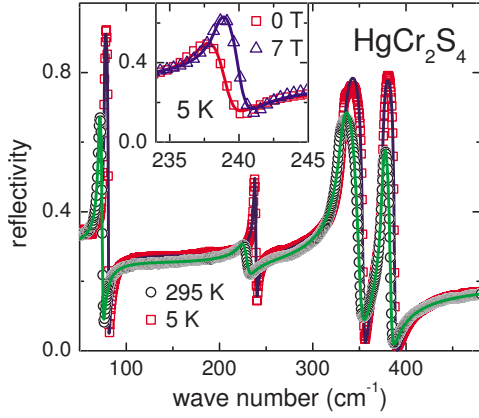


FIG. 1. (Color online) Reflectivity vs wave number in HgCr_2S_4 at 5 K (open red squares) and 295 K (open black circles). The inset shows the phonon response close to 240 cm^{-1} as measured in zero magnetic field (red open squares) and in a magnetic field of 7 T (blue open triangles). In external magnetic fields, the excitation frequency is shifted toward higher energies. The solid lines are the results of fits as described in the text.

$$\Delta\omega = \frac{-R_1\langle S_1 \cdot S_2 \rangle + R_2\langle S_1 \cdot S_3 \rangle}{\langle S_0^z \rangle^2}. \quad (16)$$

Here, R_1 and R_2 are spin dependent force constants of the lattice vibrations deduced as the squared derivatives of the exchange integrals with respect to the phonon displacements.³⁴ R_1 describes the nearest-neighbor (nn) FM and R_2 the AFM next-nearest-neighbor (nnn) exchange. Using this formalism, negative and positive frequency shifts depend on the strength of FM or AFM exchange interactions, respectively. In CdCr_2S_4 and HgCr_2S_4 , we identify the negative contributions to the eigenfrequencies with nn FM Cr-S-Cr exchange and positive contributions with nnn AFM Cr-S-Cd/Hg-S-Cr exchange. Hence, vibrations involving Cr-S bonds will predominantly be influenced by FM exchange, while eigenmodes of Cd-S or Hg-S ions will be sensitive to AFM exchange.

The temperature dependence of the phonon damping due to spin-phonon interactions has been calculated by Wesselinova and Apostolov.³⁴ These authors show that in the magnetically ordered phase, an additional contribution to the phonon damping arises due to spin-phonon interactions, which vanishes in the paramagnetic phase.

IV. EXPERIMENTAL RESULTS

A. Reflectivity measurements in zero external field

Figure 1 shows the reflectivity R of HgCr_2S_4 as measured on ceramic samples at 295 K (black circles) and at 5 K (red squares). Already this figure provides clear evidence of a significant temperature dependence of the eigenfrequencies and an enormously strong temperature dependence of damping and dielectric strength of the modes. In a normal anharmonic solid one expects an almost temperature independent dielectric strength, and on increasing temperature, eigenfrequencies should moderately decrease whereas damping in-

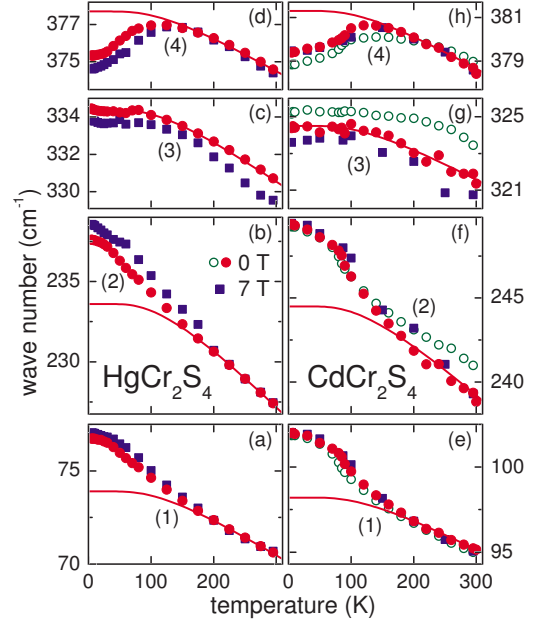


FIG. 2. (Color online) Temperature dependencies of eigenfrequencies (transverse optical modes) of HgCr_2S_4 [left frames (a)–(d)] and CdCr_2S_4 [right frames (e)–(h)]. The four phonon modes are labeled with increasing wave number. Eigenfrequencies in zero external field are shown as closed red circles, in magnetic fields of 7 T as closed blue squares. Eigenfrequencies in CdCr_2S_4 as determined in zero magnetic field in a ceramic sample are shown by open green circles. The red solid lines are fits to the eigenfrequencies in zero field assuming a purely anharmonic temperature dependence of the eigenfrequencies utilizing a fixed Debye temperature [Eq. (13), see text].

creases. The solid lines through the measured reflectivity correspond to the four-parameter fit using Eqs. (1) and (2). This fit provides a reasonable description of the experimental results. Deviations appear only at the maximum of mode 3 close to 330 cm^{-1} , which probably arise due to imperfections of the sample surface or due to multiphonon processes.

The main results of the analysis of the reflectivity spectra of ceramic HgCr_2S_4 and single-crystalline CdCr_2S_4 as a function of temperature are shown in Figs. 2 and 3. Figure 2 shows the eigenfrequencies for HgCr_2S_4 [Figs. 2(a)–2(d)] and CdCr_2S_4 [Figs. 2(e)–2(h)] and the corresponding damping of all modes [Figs. 3(a)–3(h)]. The modes j are labeled with the numbers 1–4 with increasing wave number. Only parameters of the transverse optical modes are shown.

In the right frames of Figs. 2 and 3, we also included eigenfrequencies and phonon damping for CdCr_2S_4 as obtained on high-purity ceramic samples. Ceramic CdCr_2S_4 has been investigated to determine a possible influence of the doping with Cl which cannot be fully avoided during the single-crystal growth process. With respect to the eigenfrequencies, the agreement between single-crystalline and ceramic results is reasonable. Only mode 3 shows slight deviations of the order of 1 cm^{-1} . However, we have to keep in mind that the fit of mode 3 is not perfect (see Fig. 1) and the apparent differences can probably be attributed to the fitting procedure. More significant deviations appear in the temperature dependence of the damping constants. While the

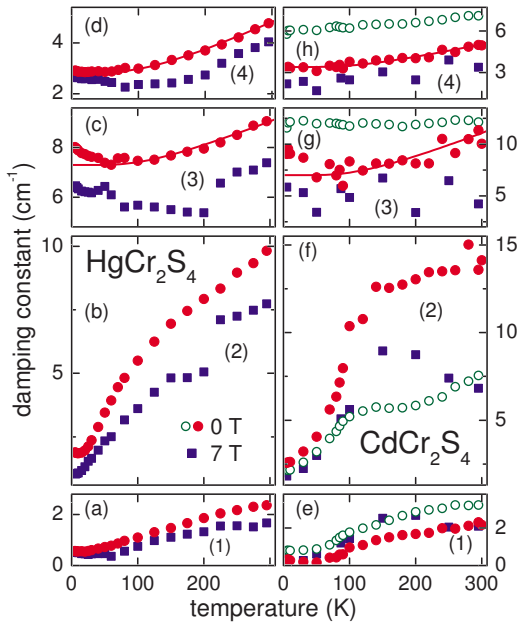


FIG. 3. (Color online) Phonon damping of the transverse optical modes versus temperature for HgCr_2S_4 [left frames (a)–(d)] and CdCr_2S_4 [right frames (e)–(h)]. Damping constants in zero external field are shown as closed red circles, in magnetic fields of 7 T as closed blue squares. Damping constants in CdCr_2S_4 as determined in a ceramic sample are shown by open green circles. The solid lines are fits assuming a purely anharmonic temperature dependence of the damping utilizing a fixed Debye temperature (see text).

general temperature dependence is rather similar, specifically modes 2 and 4 reveal rather different absolute values. Nevertheless, we conclude from these results that while a small amount of doping significantly influences the dielectric properties at low frequencies, the phonon properties seen via the reflectivity are only barely influenced. In what follows, we will only discuss the results obtained on ceramic HgCr_2S_4 and single-crystalline CdCr_2S_4 .

The eigenfrequencies for HgCr_2S_4 [Figs. 2(a)–2(d)] span a range from 70 to 377 cm^{-1} and for CdCr_2S_4 [Figs. 2(e)–2(h)] from 95 to 381 cm^{-1} . This observation indicates that the high-frequency modes in both compounds exhibit almost identical eigenfrequencies and Cr and S ions can be involved only in mode 4. The frequencies of phonon mode 1 scale with the square root of the inverse masses of mercury and cadmium, pointing toward the fact that in the low-frequency modes, mainly the closed-shell metals of the zinc group are involved. Striking similarities between antiferromagnetic HgCr_2S_4 and ferromagnetic CdCr_2S_4 can also be recognized for the temperature dependence of the damping constants. At low temperatures, the damping constants of both compounds are small for modes 1, 2, and 4 but are rather large for mode 3. Mode 2 reveals a strikingly strong temperature dependence for HgCr_2S_4 as well as for CdCr_2S_4 .

The solid lines in Figs. 2 and 3 correspond to the expected anharmonic temperature dependence of frequencies and dampings as calculated according to Eqs. (13) and (14). These curves have been derived by fitting the high-temperature ($T > 150$ K) values of the eigenfrequencies and dampings. This procedure seems to be straightforward and

correct for the eigenfrequencies of all modes in both compounds (Fig. 2). It also properly describes the temperature dependence of the phonon dampings of modes 3 and 4 for HgCr_2S_4 and CdCr_2S_4 . The temperature dependence of the damping constants of modes 1 and 2 of both compounds cannot be described in this way. For these two modes, a continuous increase of the damping is enhanced by a bump-like feature close to 150 K, which could result from structural instabilities which appear definitely far above the magnetic ordering temperatures.^{9,10,18} We would like to recall that according to theory,³⁴ one would expect additional contributions to the damping from phonon-magnon scattering in the magnetically ordered phases, which vanish in the paramagnetic states. This definitely is not observed. These strong cusplike features in the damping constants of both compounds are rather extended and definitely do neither exhibit a maximum close to T_C in CdCr_2S_4 ($T_C = 84.5$ K) nor close to 60 K in HgCr_2S_4 , where in zero external field, the strongest ferromagnetic fluctuations are observed.²⁰ Hence, we think that an explanation of the damping anomalies of mode 2 of both compounds in terms of ferromagnetic fluctuations is rather unlikely. In recent Raman scattering experiments,¹⁸ pronounced anomalies in intensity and frequency of Raman-active modes have been observed, arising at an onset temperature $T^* \approx 130$ K, which coincides with striking anomalies in the IR properties.

Already at first sight, it becomes clear that AFM HgCr_2S_4 and FM CdCr_2S_4 behave similar: The eigenfrequencies of modes 1 and 2 in both compounds reveal clear positive shifts as compared to normal anharmonic behavior, while modes 3 and 4 exhibit negative shifts when entering the magnetic phase. This again documents that in modes 3 and 4, the eigenfrequencies are determined mainly from force constants between Cr and S ions, which are coupled ferromagnetically. On the other hand, Cd/Hg-S ions are involved in the vibrations of modes 1 and 2, which are obviously strongly influenced by the AFM Cr-S-Cd/Hg-S-Cr exchange. It is important to note that the temperature dependence of the eigenfrequencies looks very similar for both compounds, despite the fact that HgCr_2S_4 reveals antiferromagnetic order below 22 K, while CdCr_2S_4 is ferromagnetic below 84.5 K. No indications of phonon splittings in antiferromagnetic HgCr_2S_4 are observable. However, both compounds show strong ferromagnetic fluctuations already at rather elevated temperatures, and it is probably this fact which explains the similarity in the temperature dependence of the phonons. Strong anomalous contributions are also observed in the temperature dependence of the damping. Modes 1 and 2 exhibit a significant decrease of the damping below 150 K for both compounds. This unusual behavior could be attributed to the onset of local polar order. On the contrary, the dampings of mode 3 slightly increase below 100 K, while mode 4 of HgCr_2S_4 and that of CdCr_2S_4 are very close to the normal temperature dependence of the damping in anharmonic solids.

The eigenfrequencies at 5 K are listed in Table I and compared to the results from LSDA+ U calculations of Fennie and Rabe.¹³ Here, we also included extrapolated eigenfrequencies ω_{70j} [see Eq. (13)], which correspond to the eigenfrequencies at 0 K in the absence of spin-phonon coupling.

TABLE I. Transversal ω_T [cm^{-1}] and longitudinal ω_L [cm^{-1}] optical eigenfrequencies of CdCr_2S_4 compared with theoretical values predicted by LSDA+ U (Ref. 13). The extrapolated eigenfrequencies at 0 K, ω_{T0j} [cm^{-1}], in the absence of spin-phonon coupling are also listed.

Mode	Expt.			LSDA+ U	
	ω_{Tj}	ω_{Lj}	ω_{T0j}	ω_{Tj}	ω_{Lj}
1	102	105	98	104	107
2	249	251	244	249	251
3	324	352	324	339	362
4	379	395	381	385	398

With the exception of mode 3, we find good agreement. From Table I, we can also infer that the frequency shift at 0 K in CdCr_2S_4 due to spin-phonon coupling $\Delta\omega_{Tj} = \omega_{Tj} - \omega_{T0j}$ is positive and of the order of 5 cm^{-1} for modes 1 and 2, but negative and significantly smaller for modes 3 and 4. The very same is true for the spin-phonon coupling in HgCr_2S_4 [Figs. 2(a)–2(d)]. This signals, as outlined above, that modes 3 and 4 exhibiting negative shifts are only weakly influenced by FM 90° Cr-S-Cr exchange, while modes 1 and 2 are strongly influenced by AFM nnn Cr-S-Cd/Hg-S-Cr exchange. This correlates nicely with calculations showing that in the vibrational pattern of modes 3 and 4, only Cr and S ions are involved, while a more complex pattern of motion, including all three types of ions, characterizes modes 1 and 2.¹³

B. Measurements in external magnetic fields

On HgCr_2S_4 ceramics and on CdCr_2S_4 single crystals, additional reflectivity measurements have been performed in external magnetic fields up to 7 T. The inset of Fig. 1 shows mode 2 of HgCr_2S_4 at 5 K in zero magnetic field compared to measurements in a field of 7 T. In an external field of 7 T, this mode is shifted to higher frequencies by an amount of approximately 1 cm^{-1} . The temperature dependencies of eigenfrequencies and damping constants as obtained in both compounds for all modes at 7 T are included in Figs. 2 and 3 (blue squares). As expected for a ferromagnet with a high ordering temperature, the eigenfrequencies remain unchanged within experimental uncertainties for CdCr_2S_4 (right frames of Fig. 2). For antiferromagnetic HgCr_2S_4 , which shows a metamagnetic transition below 1 T,²⁰ shifts of the order of 1 cm^{-1} are observed for $T < 100 \text{ K}$. The shifts are positive for modes 1 and 2 [see Figs. 2(a) and 2(b)], but negative for modes 3 and 4 [see Figs. 2(c) and 2(d)]. In mode 3 [Fig. 2(c)], the magnetic-field dependent shifts also show up at room temperature. Again we have to remind that the fits of mode 3 have some uncertainty due to a double-peak structure, and in this case, the differences of the eigenfrequencies as a function of field may signal the experimental uncertainties.

The most precise measurements of the magnetic-field dependence of the phonon eigenfrequencies can be made at a constant temperature and fixed spectrometer setting. As rep-

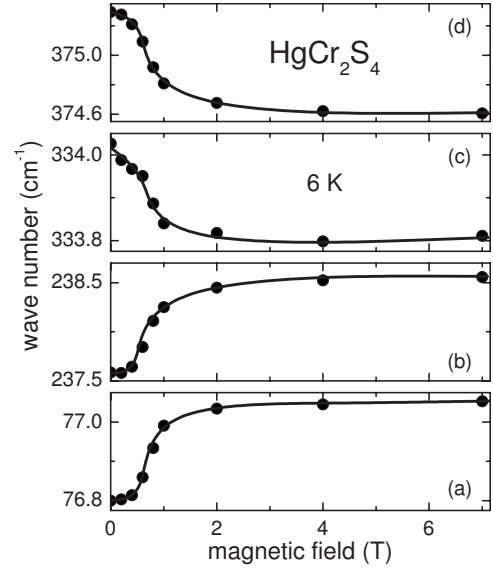


FIG. 4. Magnetic-field dependence of the eigenfrequencies of HgCr_2S_4 for modes 1 (a) to 4 (d) at 6 K. The lines are drawn to guide the eye.

resentative example, Fig. 4 shows the field dependence of all eigenmodes for HgCr_2S_4 at 6 K. As discussed above, the eigenfrequencies of modes 1 and 2 [Fig. 4(a) and 4(b)] increase, while the frequencies of modes 3 and 4 [Fig. 4(c) and 4(d)] decrease with increasing magnetic field. The frequency shifts are of the order of 1 cm^{-1} for mode 2, but smaller for the other modes. The strongest gradients for all modes appear well below 1 T, where AFM HgCr_2S_4 reveals a transition into a polarized ferromagnetic state.²⁰

Much stronger effects as a function of magnetic field are observed for the damping constants (see Fig. 3). For all modes in both compounds, we can state that while the overall temperature dependence remains similar with the same characteristic trends, we observe rather large effects in the absolute values. The reason for these significant field dependencies of the phonon damping is unclear at present, and further investigations are necessary to clarify this question.

V. ANALYSIS AND DISCUSSION

With a more elaborated analysis, we try to get insight into a possible polar short-range-order phase transition above the magnetic phase-transition temperatures in both compounds. To do so, we calculated effective plasma frequencies and LST relations. The lower frames of Fig. 5 show the Lyddane-Sachs-Teller relation for modes 1–4 for both compounds, and the upper two frames of Fig. 5 display the generalized LST relation for the static dielectric constant as calculated via Eq. (12). Within 2%, these relations remain constant for all modes. Hence, no significant softening of TO modes becomes apparent, and it is obvious that a phonon softening of the transverse acoustic modes, as observed in conventional ferroelectrics, plays no role in HgCr_2S_4 and CdCr_2S_4 . For the latter compound, this has already been concluded from first principles calculations.¹³ However, it seems worth noting that beyond experimental uncertainties, the LST relation of

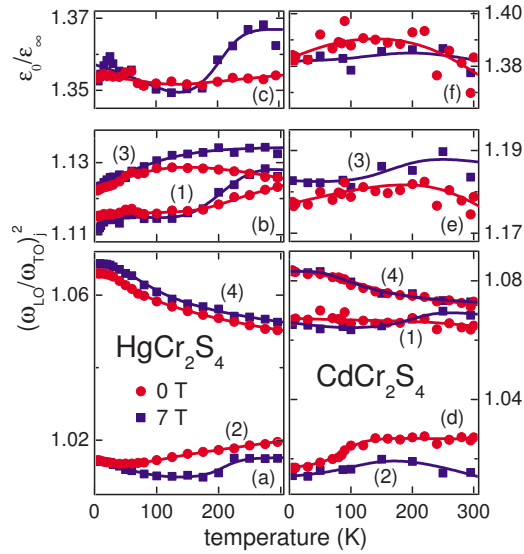


FIG. 5. (Color online) Temperature dependence of the Lyddane-Sachs-Teller relation for all modes (lower four frames) and the generalized LST relation (upper two frames) for HgCr₂S₄ [left frames (a)–(c)] and CdCr₂S₄ [right frames (d)–(f)] at zero magnetic fields (closed red circles) and in an external magnetic field of 7 T (closed blue squares). The lines are drawn to guide the eye.

mode 4 of both compounds shows a slight increase, signaling a slight hardening of LO or softening of TO modes obviously related to spin-phonon coupling. In Fig. 5, we also included the results of measurements in an external field of 7 T. Within experimental uncertainty, the results agree with those obtained at zero field.

Figure 6 shows the temperature dependence of ϵ_0 and ϵ_∞ for HgCr₂S₄ (left frame) and CdCr₂S₄ (right frame). Here, we also included the results of ϵ_0 obtained by terahertz spectroscopy at room temperature. Both dielectric constants reveal only a moderate temperature dependence. It is clear that the strong effects in the temperature dependence of the dielectric constants as observed in radio-frequency measurements^{9,10} are not mirrored in these far-infrared results. Those strong effects must be of relaxational origin and obviously are related to slow polarization fluctuations. At room temperature, ϵ_∞ is ~ 7.0 for HgCr₂S₄ and for CdCr₂S₄.

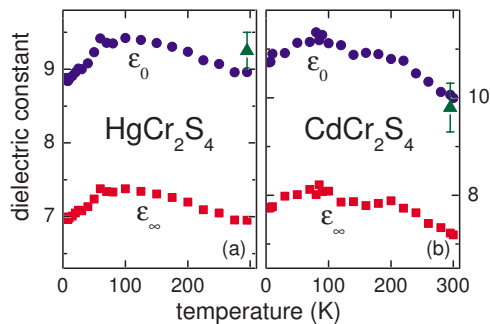


FIG. 6. (Color online) Temperature dependencies of ϵ_0 (closed blue circles) and ϵ_∞ (closed red squares) for HgCr₂S₄ (left frame) and CdCr₂S₄ (right frame). Room-temperature values of ϵ_∞ as obtained by terahertz spectroscopy are included (closed green triangles).

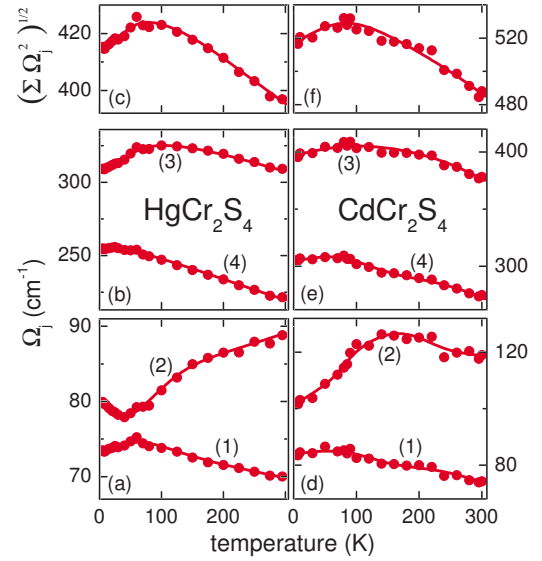


FIG. 7. (Color online) Temperature dependence of the effective plasma frequencies for modes 1–4 (lower four frames) and for the sum over all plasma frequencies (upper two frames) of HgCr₂S₄ (left frames) and CdCr₂S₄ (right frames). The lines are drawn to guide the eye.

For HgCr₂S₄, ϵ_∞ has also been determined by Lutz *et al.*²³ as 7.4, compared to 8.5 as obtained by Wakamura and Arai.¹⁹ For CdCr₂S₄, room-temperature values of $\epsilon_\infty = 6.9$ (Ref. 23), 7.6 (Ref. 19), and 7.84 (Ref. 25) have been reported. In insulating solids, the dielectric constant at frequencies beyond the ionic vibrations is determined by the electronic polarizability and the band gap. The electronic polarizability is expected to be somewhat larger in the mercury compound and despite minor effects due to thermal expansion practically temperature independent. However, ϵ_∞ also scales with the inverse squared band gap. The band gap is of the order of 1.4 eV for HgCr₂S₄ with a smooth redshift on decreasing temperature.³⁵ In CdCr₂S₄ at room temperature, the band gap has been estimated as 1.57 eV, exhibiting an unusual blueshift on decreasing temperatures.³⁶ These band gaps could not explain the observed temperature dependence of ϵ_∞ of the two compounds under consideration, which are very similar and suggest a redshift of the band edges from room temperature down to 100 K and a subsequent blueshift in the ferromagnetic phase (CdCr₂S₄) or in the state dominated by ferromagnetic fluctuations (HgCr₂S₄). Indeed, it has been suggested that these reports on the band gaps in the chromium spinels are heavily influenced by the Cr³⁺ crystal field excitations and do not represent the true electronic band edges.³⁷

In a second step, using Eqs. (1) and (7), we calculated the effective ionic plasma frequencies which, aside from thermal expansion corrections, only depend on the effective charges of the ions under consideration. The lower four frames of Fig. 7 show the temperature dependence of the plasma frequencies for HgCr₂S₄ and CdCr₂S₄ for all modes, and the upper two frames indicate the sum over all plasma frequencies in zero external magnetic field. The plasma frequencies of both compounds for all modes except for mode 2 show a moderate increase on decreasing temperature, some saturate

or go through a slight maximum close to 100 K. These effects are of the order of 10%. The temperature dependence of mode 2 of both compounds is significantly different and strongly decreases below 150 K. In CdCr_2S_4 , the overall effect of this mode is of the order of 25%, indicating strongly decreasing effective charges toward low temperatures. This can only be explained assuming strong charge transfer and/or that the character of the bonds changes considerably. It could be a first experimental hint that charge ordering phenomena are responsible for the appearance of local polar order. Local charge order is thought to be responsible for the local polar state in La:SrMnO_3 (Ref. 38) and charge-stripe order is the origin of electronic ferroelectricity in LuFe_2O_4 .³⁹ The sum over all effective ionic plasma frequencies is dominated by the strongest modes 3 and 4 and reveals the overall behavior with a shallow maximum close to 100 K. The larger ($\approx 25\%$) plasma frequency of CdCr_2S_4 as compared to the mercury compound indicates a stronger ionicity for the former compound, a fact that also follows from general considerations. According to Pauling's values of electronegativity, both Cr-S and Hg-S form rather mixed bonds, however, with a significant increase of covalency for the latter.

The plasma frequencies of CdCr_2S_4 , as derived from these experiments at 5 K, can be compared to those calculated by Fennie and Rabe¹³ in their LSDA+ U approach. Good agreement is found for modes 1–3; however, for mode 4 at low temperatures, we experimentally determined $\Omega=309\text{ cm}^{-1}$, while theoretically, 202 cm^{-1} has been calculated. In addition, from our experiments, we determined $\Delta\epsilon$ [Eq. (3)] of the order of 2.9 at 5 K compared to the theoretical value of 2.3. Our value is in good agreement with the result by Wakamura *et al.*,²⁴ who found $\Delta\epsilon=2.8$. Corresponding to the smaller plasma frequencies and to the higher covalency, $\Delta\epsilon$ for HgCr_2S_4 is significantly smaller when compared to CdCr_2S_4 and is of the order of 2 for all temperatures [see Fig. 6(a)].

With the experimentally determined effective plasma frequencies as documented in Fig. 7, we tried to get some insight into the bonding of HgCr_2S_4 and CdCr_2S_4 using Eqs. (10) and (11). Utilizing Eq. (10), we can directly calculate the effective plasma frequencies of both compounds assuming the nominal valencies Z with $\text{Hg}^{2+}/\text{Cd}^{2+}$, Cr^{3+} , and S^{2-} . For 300 K and with an averaged ϵ_∞ , we calculated theoretical ionic plasma frequencies of 1568 cm^{-1} for HgCr_2S_4 and of 1517 cm^{-1} for CdCr_2S_4 . These values have to be compared with the results shown in Figs. 7(c) and 7(f), where we find an average value of the effective plasma frequency of 415 cm^{-1} for the mercury and of 515 cm^{-1} for the cadmium compound. Hence, we can state that the overall ionicity, i.e., the normalized effective charge, Z^*/Z , amounts to 26% in HgCr_2S_4 and 34% in CdCr_2S_4 . Proceeding one step further, one may calculate the effective charges of the different ions in both compounds combining Eqs. (10) and (11). However, due to the fact that three unknown quantities, namely, Z_k^* for each ion, correspond to two equations only, we have to make another *ad hoc* assumption, namely, that the electronegativity of the closed-shell transition metal equals that of Cr. In other words, the relation of the effective charges has to be $Z_{\text{Hg/Cd}}^*=2/3Z_{\text{Cr}}^*$, or equivalently, $Z_{\text{Hg/Cd}}^*=-Z_{\text{S}}^*$. This produces an average reduction of the effective charges of all ions according

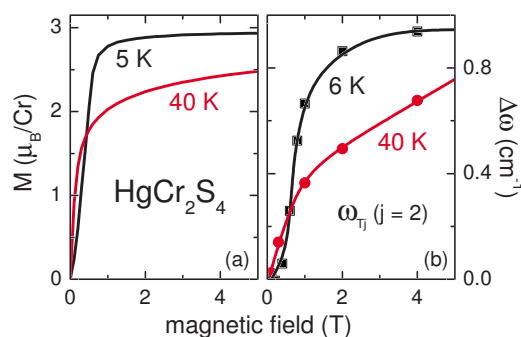


FIG. 8. (Color online) (a) Magnetic-field dependence of the magnetization in HgCr_2S_4 at 5 and 40 K, which is well below and above the antiferromagnetic ordering temperature at 22 K. (b) Magnetic-field dependence of the frequency shift of the transverse optical phonon mode 2 at 6 and 40 K. The lines are drawn to guide the eye.

to the values determined from the overall theoretical and experimental plasma frequencies. We achieve the effective charges for (Hg/Cd, Cr, S) as (0.52, 0.78, -0.52) for the mercury and (0.66, 0.99, -0.66) for the cadmium compound.

The effective plasma frequencies as obtained in an external magnetic field of 7 T are not shown. The magnetic-field dependence of the far-infrared intensities does not scale significantly enough with the external magnetic field to compare results on different runs with different adjustments of the spectrometer. However, as outlined above, the sensitivity is good enough to search for changes of eigenfrequencies, dampings, and intensities at a given temperature as a function of external magnetic field without changing the instrument setting. A representative example of such a measurement is given in the inset of Fig. 1. With a given setting and at constant temperature, we measured the magnetic-field dependence of phonon mode 2 in HgCr_2S_4 at 6 K in the AFM state ($T < T_N$) and at 40 K in the paramagnetic state ($T > T_N$). The results are shown in the right frame of Fig. 8 and compared to the magnetization at similar temperatures [Fig. 8(a)]. The frequency shift of the phonon mode is strongly correlated with the magnetization, even revealing a strong metamagnetic transition in the AFM state. Thus, the mutual correspondence of magnetization and phonon shift documents a significant magnetoelectric coupling even at optical frequencies.

VI. CONCLUDING REMARKS

Our far-infrared study of HgCr_2S_4 and CdCr_2S_4 was in part motivated to search for experimental evidence for a polar phase transition close to 100 K, above the onset of magnetic order. The onset of relaxor ferroelectricity has been brought up in Refs. 9 and 10 and has reinforced old speculations of polar distortions in spinel compounds at elevated temperatures.^{11,12} For CdCr_2S_4 negative thermal expansion below 150 K,^{40,41} the broadening of Bragg reflections in x-ray diffraction experiments at temperatures above the ferromagnetic phase transition at T_C (Ref. 40) provided some experimental evidence for short-range structural distortions

close to 150 K. In recent synchrotron radiation experiments, a (200) reflection, which is forbidden in the spinel structure, showed up below 200 K with increasing intensity toward 0 K.⁴¹ The onset of polar distortions has also been claimed in recent Raman scattering experiments,¹⁸ where pronounced anomalies in the Raman modes appear below a characteristic temperature $T^* \approx 130$ K.

We can certainly state that in accord with recent LSDA + U calculations,¹³ we found no evidence for soft-mode behavior, which usually is a fingerprint for ferroelectricity in proper ferroelectrics. This statement is based on the observations as presented in Fig. 2, but also from the almost constant LST relations as presented in Figs. 5(c) and 5(f). However, we would like to recall that the soft-mode concept, which couples a soft transverse mode to a divergent static dielectric susceptibility in multiferroics, may not be the adequate description. For the perovskite-type family of multiferroics, it has been shown theoretically^{42,43} and proven experimentally^{44,45} that electromagnons, i.e., coupled spin-phonon excitations, are the relevant excitations. The ferroelectric transition in these compounds is then rather driven by a soft magnetic excitation.

Nevertheless, in this work, we provide evidence for strong spin-phonon coupling. The onset of these effects (Figs. 2 and 3) can certainly be detected far above the magnetic transition temperature, and it is unlikely that these effects are driven by ferromagnetic fluctuations. In both compounds, mode 2 behaves rather unusual, with a broad cusp in the temperature dependence of the damping constant and specifically a significant anomaly in the plasma frequency. Both anomalies are located close to 150 K.

In summary, the main outcomes of this work are the following:

(i) Within the experimental resolution, there is no splitting of phonon modes in AFM HgCr₂S₄, and it behaves very

similar like FM CdCr₂S₄, demonstrating that both compounds are dominated by ferromagnetic exchange interactions.

(ii) There are strong frequency shifts in the phonon modes from normal anharmonic behavior, which are positive for modes 1 and 2, but negative for modes 3 and 4. For both compounds, these shifts appear well above the onset of magnetic order. For CdCr₂S₄, a detailed phonon study in zero magnetic field on ceramic samples has been reported already by Wakamura and Arai some decades ago.¹⁹ The results of both studies are in good agreement, however, with differences in the temperature dependence of the dielectric constants ϵ_0 and ϵ_∞ .

(iii) In AFM HgCr₂S₄, we find significant shifts of the eigenfrequencies by external magnetic fields, which scale perfectly well with the macroscopic magnetization.

(iv) The plasma frequencies of both compounds reveal a moderate increase on decreasing temperature with the exception of mode 2, which exhibits a strong decrease below 150 K.

(v) The Lyddane-Sach-Teller relations of all modes behave rather normal as function of temperature and magnetic field. Within experimental uncertainty, only mode 4 reveals a moderate increase in the LST relation in both compounds.

(vi) The overall ionicity as determined from the sum over all ionic effective plasma frequencies is 28% for HgCr₂S₄ and is 33% for CdCr₂S₄, under the assumption that the normal valency would produce 100% ionic bonds.

ACKNOWLEDGMENTS

Stimulating discussions and helpful comments by P. Lemmens are gratefully acknowledged. This work partly was supported by the Deutsche Forschungsgemeinschaft through the German Research Collaboration SFB 484 (University of Augsburg).

¹P. K. Baltzer, P. J. Wojtowicz, M. Robbins, and E. Lopatin, Phys. Rev. **151**, 367 (1966).

²T. Rudolf, Ch. Kant, F. Mayr, J. Hemberger, V. Tsurkan, and A. Loidl, New J. Phys. **9**, 76 (2007).

³A. P. Ramirez, in *Handbook of Magnetic Materials*, edited by K. H. J. Buschow (Elsevier Science, New York/North-Holland, Amsterdam, 2001), Vol. 13, p. 423.

⁴Y. Yamashita and K. Ueda, Phys. Rev. Lett. **85**, 4960 (2000).

⁵O. Tchernyshyov, R. Moessner, and S. L. Sondhi, Phys. Rev. Lett. **88**, 067203 (2002).

⁶A. B. Sushkov, O. Tchernyshyov, W. Ratcliff II, S. W. Cheong, and H. D. Drew, Phys. Rev. Lett. **94**, 137202 (2005).

⁷J. Hemberger, T. Rudolf, H.-A. Krug von Nidda, F. Mayr, A. Pimenov, V. Tsurkan, and A. Loidl, Phys. Rev. Lett. **97**, 087204 (2006).

⁸T. Rudolf, Ch. Kant, F. Mayr, J. Hemberger, V. Tsurkan, and A. Loidl, Phys. Rev. B **75**, 052410 (2007).

⁹J. Hemberger, P. Lunkenheimer, R. Fichtl, H.-A. Krug von Nidda, V. Tsurkan, and A. Loidl, Nature (London) **434**, 364 (2005).

¹⁰S. Weber, P. Lunkenheimer, R. Fichtl, J. Hemberger, V. Tsurkan,

and A. Loidl, Phys. Rev. Lett. **96**, 157202 (2006).

¹¹N. W. Grimes, J. Phys. C **6**, L78 (1973); N. W. Grimes, Philos. Mag. **26**, 1217 (1972); L. Hwang, A. H. Heuer, T. E. Mitchell, *ibid.* **28**, 241 (1973); A. H. Heuer and T. E. Mitchell, J. Phys. C **8**, L541 (1975).

¹²H. Schmid and E. Ascher, J. Phys. C **7**, 2697 (1974).

¹³C. J. Fennie and K. M. Rabe, Phys. Rev. B **72**, 214123 (2005).

¹⁴J. Hemberger, P. Lunkenheimer, R. Fichtl, S. Weber, V. Tsurkan, and A. Loidl, Phase Transitions **79**, 1065 (2006).

¹⁵V. Tsurkan (unpublished).

¹⁶A. J. Bosman and C. Crevecoeur, J. Phys. Chem. Solids **29**, 109 (1968); C. Crevecoeur and H. J. de Wit, Solid State Commun. **6**, 843 (1968).

¹⁷P. Lunkenheimer, A. Loidl, C. R. Ottermann, and K. Bange, Phys. Rev. B **44**, 5927 (1991).

¹⁸V. Gnezdilov, P. Lemmens, Yu. G. Pashkevich, P. Scheib, Ch. Payen, K. Y. Choi, J. Hemberger, A. Loidl, and V. Tsurkan, arXiv:cond-mat/0702362 (unpublished).

¹⁹K. Wakamura and T. Arai, J. Appl. Phys. **63**, 5824 (1988).

²⁰V. Tsurkan, J. Hemberger, A. Krimmel, H.-A. Krug von Nidda, P.

- Lunkenheimer, S. Weber, V. Zestrea, and A. Loidl, *Phys. Rev. B* **73**, 224442 (2006).
- ²¹L. C. Chapon, P. G. Radaelli, Y. S. Hor, M. T. F. Telling, and J. F. Mitchell, arXiv:cond-mat/0608031 (unpublished); P. G. Radaelli and L. C. Chapon, *Phys. Rev. B* **76**, 054428 (2007).
- ²²B. Gorshunov, A. Volkov, I. Spektor, A. Prokhorov, A. Mukhin, M. Dressel, S. Uchida, and A. Loidl, *Int. J. Infrared Millim. Waves* **26**, 1217 (2005).
- ²³H. D. Lutz, G. Wäschenbach, G. Kliche, and H. Haeuseler, *J. Solid State Chem.* **48**, 196 (1983); H. D. Lutz, B. Müller, and H. J. Steiner, *ibid.* **90**, 54 (1991); J. Zwinscher and H. D. Lutz, *ibid.* **118**, 43 (1995); J. Zwinscher and H. D. Lutz, *J. Alloys Compd.* **219**, 103 (1995).
- ²⁴K. Wakamura, T. Ogawa, and T. Arai, *Jpn. J. Appl. Phys.* **19**, 249 (1980).
- ²⁵T. H. Lee, *J. Appl. Phys.* **42**, 1441 (1971).
- ²⁶A. Kuzmenko, RefFIT, Version 1.2.44, University of Geneva, 2006, <http://optics.unige.ch/alexey/reffit.html>
- ²⁷J. F. Scott, *Phys. Rev. B* **4**, 1360 (1971).
- ²⁸K. Wakamura and T. Arai, *Phys. Rev. B* **24**, 7371 (1981).
- ²⁹R. A. Cowley, *Adv. Phys.* **12**, 421 (1963).
- ³⁰W. Baltensperger and J. S. Helman, *Helv. Phys. Acta* **41**, 668 (1968).
- ³¹W. Baltensperger, *J. Appl. Phys.* **41**, 1052 (1970).
- ³²P. Brüesch and F. D'Ambrogio, *Phys. Status Solidi B* **50**, 513 (1972).
- ³³D. J. Lockwood and M. G. Cottam, *J. Appl. Phys.* **64**, 5876 (1988).
- ³⁴J. M. Wesselinowa and A. T. Apostolov, *J. Phys.: Condens. Matter* **8**, 473 (1996).
- ³⁵H. W. Lehmann and G. Harbeke, *Phys. Rev. B* **1**, 319 (1970).
- ³⁶G. Harbeke and H. Pinch, *Phys. Rev. Lett.* **17**, 1090 (1966).
- ³⁷S. Wittekoek and P. F. Bongers, *Solid State Commun.* **7**, 1719 (1969).
- ³⁸R. F. Mamin, I. K. Bdikin, and A. L. Kholkin, arXiv:0706.1164 (unpublished).
- ³⁹Y. Zhang, H. X. Yang, C. Ma, H. F. Tian, and J. Q. Li, *Phys. Rev. Lett.* **98**, 247602 (2007).
- ⁴⁰H. Göbel, *J. Magn. Magn. Mater.* **3**, 143 (1976).
- ⁴¹A. Krimmel (unpublished).
- ⁴²H. Katsura, A. V. Balatsky, and N. Nagaosa, *Phys. Rev. Lett.* **98**, 027203 (2007).
- ⁴³I. E. Chupis, *Low Temp. Phys.* **33**, 715 (2007).
- ⁴⁴A. Pimenov, A. A. Mukhin, V. Yu. Ivanov, V. D. Travkin, A. M. Balbashov, and A. Loidl, *Nat. Phys.* **2**, 97 (2006).
- ⁴⁵A. Pimenov, T. Rudolf, F. Mayr, A. Loidl, A. A. Mukhin, and A. M. Balbashov, *Phys. Rev. B* **74**, 100403(R) (2006).